Cellular and Molecular Life Sciences (2020) 77:5189–5205
https://doi.org/10.1007/s00018-019-03440-7

ORIGINAL ARTICLE

GPR50-Ctail cleavage and nuclear translocation: a new signal transduction mode for G protein-coupled receptors

Raise Ahmad[1] · Olivier Lahuna[1] · Anissa Sidibe[1] · Avais Daulat[1] · Qiang Zhang[1] · Marine Luka[1] · Jean-Luc Guillaume[1] · Sarah Gallet[2] · François Guillonneau[1] · Juliette Hamroune[1] · Sophie Polo[3] · Vincent Prévot[2] · Philippe Delagrange[4] · Julie Dam[1] · Ralf Jockers[1]

Received: 14 July 2019 / Revised: 21 November 2019 / Accepted: 23 December 2019 / Published online: 3 January 2020

Abstract

Transmission of extracellular signals by G protein-coupled receptors typically relies on a cascade of intracellular events initiated by the activation of heterotrimeric G proteins or β-arrestins followed by effector activation/inhibition. Here, we report an alternative signal transduction mode used by the orphan GPR50 that relies on the nuclear translocation of its carboxyl-terminal domain (CTD). Activation of the calcium-dependent calpain protease cleaves off the CTD from the transmembrane-bound GPR50 core domain between Phe-408 and Ser-409 as determined by MALDI-TOF-mass spectrometry. The cytosolic CTD then translocates into the nucleus assisted by its 'DPD' motif, where it interacts with the general transcription factor TFII-I to regulate c-fos gene transcription. RNA-Seq analysis indicates a broad role of the CTD in modulating gene transcription with ~ 8000 differentially expressed genes. Our study describes a non-canonical, direct signaling mode of GPCRs to the nucleus with similarities to other receptor families such as the NOTCH receptor

Keywords GPCR · Orphan · Calpain · GPR50 · Proteolytic cleavage · Signal transduction

Introduction

G protein-coupled receptors (GPCRs) constitute the largest membrane receptor family in humans. They respond to a wide variety of extracellular molecules and play a crucial role in cell-to-cell communication by transmitting extracellular signals into cells. The current paradigm of intracellular signal transduction by GPCRs relies on a multistep pathway initiated by the engagement of heterotrimeric G proteins or β-arrestins, followed by the generation of soluble second messengers and activation/inhibition of various effectors [1]. Among the approximately 400 non-odorant GPCRs in humans, more than 100 are orphans for which no endogenous ligand has been identified yet. GPR50 is one of these orphans. In the absence of any known ligand for GPR50, we proposed in 2006 the existence of ligand-independent functions for GPR50 such as the allosteric regulation of other proteins/receptors through their interaction with GPR50 in common protein complexes [2, 3]. The discovery of the molecular complex of GPR50 with the melatonin MT_1 receptor, in which GPR50 negatively regulates the function of MT_1 [4], and the complex of GPR50 with the transforming growth factor-β (TGFβ) type I receptor (TβRI), in which GPR50 renders TβRI constitutively active [5], provided experimental support for this hypothesis. GPR50 is composed of the canonical seven-transmembrane domain (7TM) and a long intracellular carboxyl-terminal domain (CTD) of approximately 300 amino acids. The long CTD has been added to the *GPR50* gene during evolution by replacing the stop codon present in species such as

Electronic supplementary material The online version of this article (https://doi.org/10.1007/s00018-019-03440-7) contains supplementary material, which is available to authorized users.

✉ Ralf Jockers
ralf.jockers@inserm.fr

1 Université de Paris, Institut Cochin, CNRS, INSERM, 22 rue Méchain, 75014 Paris, France

2 Jean-Pierre Aubert Research Center, U837 Lille, France

3 Epigenetics and Cell Fate Centre, UMR7216, CNRS, Paris Diderot University, Paris, France

4 Pôle D'Innovation Thérapeutique Neuropsychiatrie, Institut de Recherches Servier, 125 Chemin de Ronde, 78290 Croissy, France

zebrafish, chicken and platypus by the sequence of the long CTD in therian mammals such as mice and humans [6, 7]. Little is known about the function of the CTD apart from its sequence homology with the DNA-directed RNA polymerase II [6]. Furthermore, circumstantial evidence suggests that the CTD of GPR50 participates in the effect of GPR50 on TβRI activation [5], glucocorticoid receptor signaling [8] and neuronal differentiation possibly through notch and wnt/β-catenin signaling [9]. Detection of two bands at apparent molecular weights of ~ 70 and ~ 35 kDa by Western blots of HEK293 cells expressing the C-terminal myc-tagged mouse GPR50 with anti-Myc antibodies suggested the generation of a 35 kDa proteolytic cleavage fragment corresponding to the CTD of GPR50 in addition to the ~ 70 kDa full-length mouse receptor [8].

Here, we show that the proteolytic cleavage of the CTD of GPR50 occurs in vivo in the mouse brain and involves the calcium-dependent cysteine protease calpain. The generated truncated CTD (tCTD) composed of amino acids 409–617 then translocates into the nucleus where it interacts with the ubiquitously expressed transcription factor TFII-I to promote TFII-I-dependent c-fos gene transcription. Transcriptomic (RNA-Seq) analysis revealed the broad impact of the ectopic expression of tCTD on gene transcription in HEK293 cells with enrichment in canonical pathways/upstream regulators related to the transcriptional/cell cycle machinery.

Results

Detection of the truncated carboxyl-terminal domain of GPR50

The migration pattern of the GPR50 protein on SDS-PAGE is complex due to its high hydrophobicity, being a seven transmembane protein, and its tendency to form oligomers. When mouse brain lysates from wild-type or GPR50 knockout mice were analyzed for GPR50 expression with an antibody recognizing the last 13 amino acids of GPR50 intracellular CTD [10], a predominant band at ~ 70 kDa was observed corresponding to the predicted size of the GPR50 monomer (Fig. 1, left panel). Additional bands were observed at ~ 140 kDa and higher corresponding to GPR50 dimers and oligomers, respectively, and at ~ 35 kDa, most likely corresponding to the tCTD of GPR50. These bands were specific to GPR50, since they were absent in brain lysates from GPR50 knockout (GPR50KO) mice (Fig. 1 left panel). A similar migration pattern composed of monomers, dimers and the 35 kDa tCTD was observed in the human lung carcinoma cell line (NCI-H520) expressing GPR50 endogenously [5] and in transfected HEK293 cells expressing the human GPR50 (Fig. 1, middle and right panel). The extent of cleavage is estimated to range from 2 to 10%. The N-terminal fragment corresponding to the GPR50 core deleted of its tCTD was detected at ~ 45 kDa with an N-terminally HA-tagged GPR50 construct (Suppl Fig. 1b). Taken together, our results show the presence of a tCTD

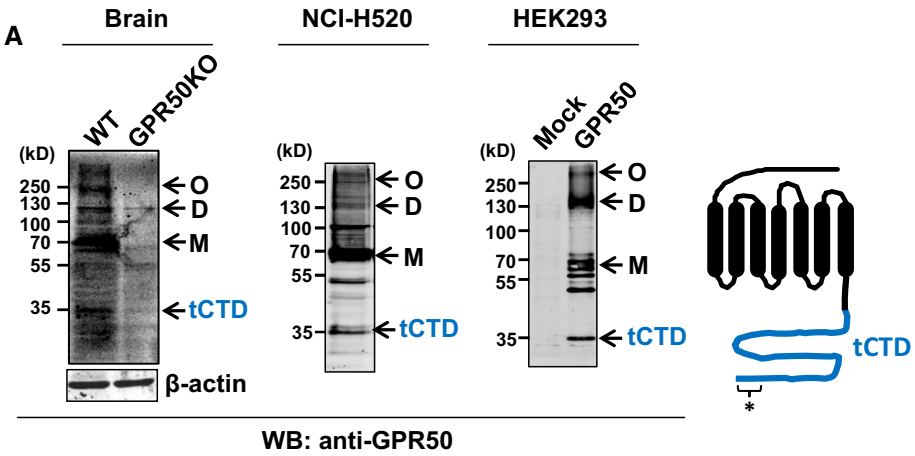

Fig. 1 Expression of full-length and truncated forms of GPR50. Western blots showing different forms of GPR50 in mouse brain lysates of WT and GPR50 knockout (KO) mice (left), and human lung carcinoma cells (NCI-H520) (middle) and HEK293 cells (right) transfected with empty (mock) or GPR50 expression plasmids. An anti-GPR50 antibody recognizing the last 13 amino acids of GPR50 was used as primary antibody. *M* monomer, *D* dimer, *O* higher molecular weight oligomers, *tCTD* truncated C-terminal domain. Asterisk indicates the location of the epitope recognized by the anti-GPR50 antibody. Representative results are shown. Similar results were obtained in at least two additional experiments. See also Supplementary Fig. 1

of GPR50 in addition to the full-length membrane-bound GPR50 in mouse and human in various cellular contexts.

Calpain cleaves the tCTD of GPR50 in a calcium-dependent manner

Considering the systematic detection of the tCTD of GPR50 in cell and tissue lysates, we hypothesized that the tCTD is generated through controlled proteolytic cleavage. Tandem affinity purification of GPR50 complexes [11] identified calpain protease as an interacting partner of GPR50 (data not shown), suggesting the involvement of calpain for proteolytic cleavage of GPR50. To identify the protease involved, HEK293 cells expressing the human GPR50 were treated with various protease inhibitors including calpain inhibitors, to prevent the generation of the tCTD. Whereas pepstatin, E64d and lactacystin were ineffective, several serine/cysteine protease inhibitors known to inhibit calpain protease activity (leupeptin, AEBSF, the mixed proteasome/calpain inhibitor MG132), as well as specific calpain inhibitors [ALLN (calpain 1) and ALLM (calpain 2)] prevented the generation of the tCTD fragment (Fig. 2a). The inhibitory effect of MG132 most likely relies on the inhibition of calpains and not of the proteasome in agreement with the absence of the effect of the proteasome-specific lactacystin. Furthermore, the inhibition of lysosomal enzyme activity by treating cells with chloroquine did not impair the generation of the tCTD and did not prevent the inhibitory action of AEBSF, ALLN, ALLM and MG132, indicating that lysosomes are not involved in the generation or degradation of the tCTD (Fig. 2b). The effectiveness of the ALLN calpain inhibitor in preventing the formation of the tCTD was recapitulated in the NCI-H520 cell model (Fig. 2c). The protease activity of calpain being calcium dependent, its involvement in forming the tCTD was further studied by increasing intracellular Ca^{2+} levels of NCI-H520 cells with ionomycin leading to a 2.96 ± 0.38-fold increase in tCTD generation ($^{*}p = 0.016$: two-tailed unpaired *t* test) (Fig. 2d) or incubating NCI-H520 cell lysates in vitro with recombinant calpain 1 and calcium (Fig. 2e). Both conditions rapidly (within 5 min) increased tCTD formation in an ALLN-dependent manner. In the absence of exogenous calcium, recombinant calpain was inactive in NCI-H520 cell lysates (Fig. 2e).

Similar results were obtained with an engineered GPR50 construct encompassing the entire CTD of GPR50 (full-length CTD or flCTD; apparent MW ~ 45kD; Suppl Fig. 2a) in the in vitro calpain 1 assay (Fig. 2f, Suppl Fig. 2b) and in intact cells (Suppl Fig. 2c). The kinetics of tCTD generation were slower for the flCTD than for the full-length GPR50, most likely indicating that the soluble flCTD is a poorer calpain substrate than GPR50. Altogether, this indicates that the cleavage can occur independently of the membrane-associated GPR50 core domain and involves the same family of protease(s). To exclude any contribution of GPR50 activation in the generation of the tCTD, either by an unknown ligand present in the serum or constitutive activity of GPR50, HEK293 cells expressing GPR50 were treated with pertussis toxin (Gαi inhibitor) or YM254890 (Gαq inhibitor), two typical transmitters of GPCR activation, or were serum starved for up to 24 h. These treatments had no effect on the generation of the tCTD arguing against the involvement of any GPR50 activity mediated by Gαi or Gαq or the serum in the proteolytic cleavage (Suppl Fig. 2d). To determine the impact of calcium signaling on the generation of the tCTD triggered by other GPCRs, we coexpressed GPR50 with the Gq-coupled muscarinic M1 or serotonin 5-HT_{2C} receptors. Stimulation of both receptors (15 min) decreased the amount of generated tCTD (Suppl Fig. 2e). We also asked the question whether receptors known to interact with GPR50 such as the melatonin MT_1 receptor and TβRI modulate the ability of calpain to cleave GPR50. Whereas co-expression and activation of MT_1 had no effect, TβRI increased the generation of the tCTD with a further increase upon TGFβ stimulation (Suppl Fig. 2e).

Collectively, our results indicate that GPR50 is subject to proteolytic cleavage by calpain proteases in a calcium-dependent manner. The soluble flCTD alone is a calpain substrate and cleavage can be modulated by TβRI possibly through trans-conformational changes within a GPR50/TβRI complex.

Identification of calpain cleavage site in GPR50 by MALDI-TOF-MS analysis

Bioinformatic analysis of the human GPR50 sequence (NCBI sequence NP_004215.2) with two calpain cleavage site prediction softwares revealed the presence of four potential cleavage sites in the CTD with a high confidence score (Suppl Fig. 3). The expression of GPR50 deletion mutants spanning the four predicted cleavage sites (GPR50ΔC1 (Δ396–405), GPR50ΔC2 (Δ406–412), GPR50ΔC3 (Δ396–412), GPR50ΔC4 (Δ469–477) (Fig. 3a) showed that the tCTD was still generated in GPR50ΔC1 and GPR50ΔC4 mutants (Fig. 3b). Conversely, tCTD was absent in GPR50ΔC2 and GPR50ΔC3 mutants, both having the putative SVF/SHSK cleavage site in common, suggesting the involvement of the latter in the proteolysis releasing the tCTD (Fig. 3b).

To further validate our results, we used the synthetic peptide YK17 (YRKSASTHHKSVFSHSK) corresponding to the region deleted in the GPR50ΔC3 mutant (Fig. 3a) to compete with the cleavage of the tCTD from full-length GPR50 by recombinant calpain 1 in NCI-H520 cell lysates. Peptide YK17 inhibited in a time- and concentration-dependent manner the generation of the tCTD, whereas the control peptide AA17 (ARAHARDQAREQDRAHA)

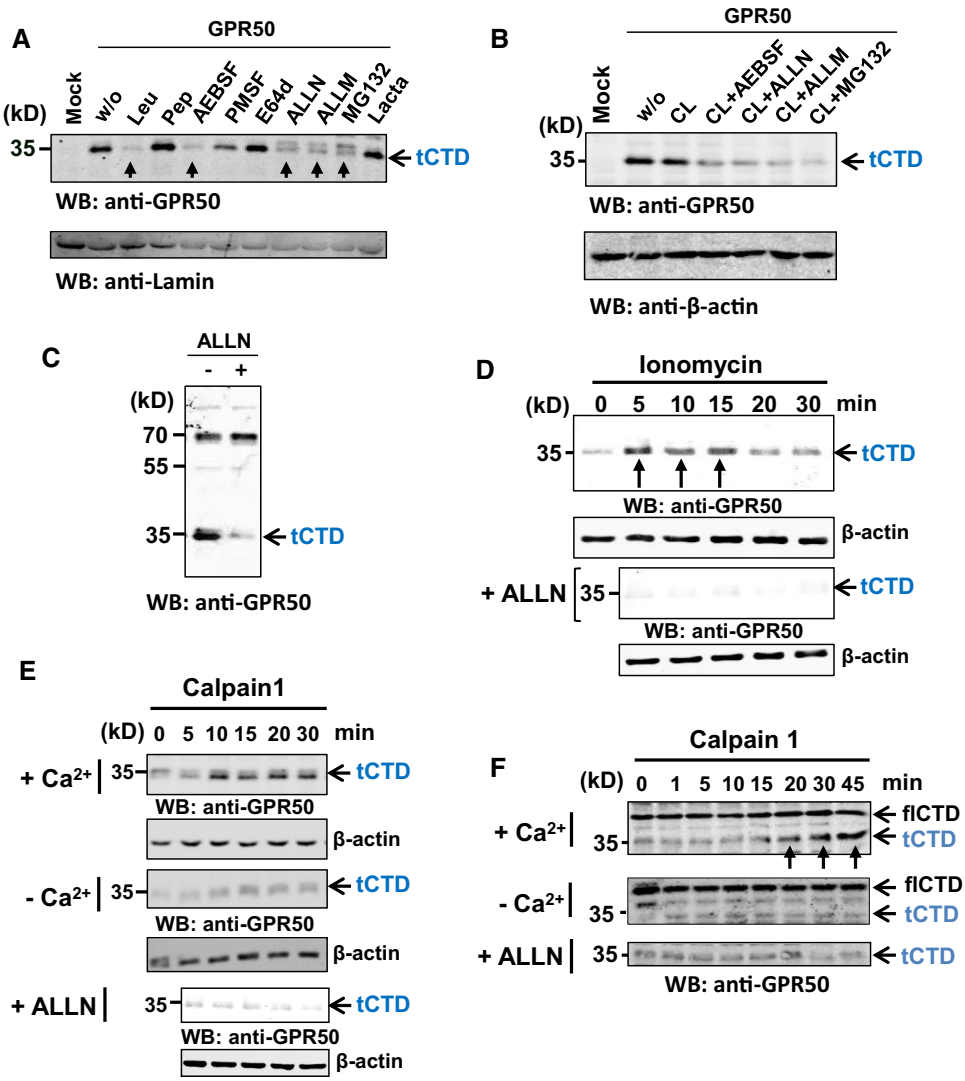

Fig. 2 The truncated CTD of GPR50 is generated by proteolytic cleavage by calpain. Western blots showing abrogation of the generation of the truncated form of GPR50 (tGPR50) in HEK293 cells expressing the full-length GPR50 (**a**, **b**) or in human lung carcinoma cells (NCI-H520) expressing GPR50 endogenously (**c**) and treated overnight with the indicated serine/cysteine protease inhibitors in the absence (**a**, **c**) or presence of the lysosomal inhibitor chloroquine (CL, 25 µM; O/N) (**b**) (w/o, without inhibitor; Leu, Leupeptin 50 µM; Pep, Pepstatin 50 µM; ALLN, calpain 1 inhibitor 10 µM; ALLM, calpain 2 inhibitor 10 µM; E64d, thiol and cathepsin inhibitor 25 µM; Lacta, lactacystin 10 µM; MG132 10 µM proteasome inhibitor). Arrows indicate abrogation of tCTD generation. Western blots showing time-dependent generation of the tCTD in intact NCI-H520 cells following incubation with ionomycin (5 µM) (**d**) or cell lysates prepared from NCI-H520 cells (**e**) or HEK293 cells expressing the entire CTD of GPR50 flCTD (**f**). Cell lysates were supplemented with recombinant calpain 1 (1 U/mg protein) and 100 µM $CaCl_2$ unless in -Ca^{2+} control conditions. Cells were pretreated or not with calpain 1 inhibitor (ALLN;10 µM; 1 h). Arrows indicate generation of tCTD. Representative results are shown for all panels. Similar results were obtained in at least two additional experiments. See also Supplementary Fig. 2

derived from another GPR50 region (Suppl Fig. 3c) was without effect (Fig. 3c). The precise cleavage site in peptide YK17 was determined by MALDI-TOF-mass spectrometry (MALDI-TOF-MS) upon treatment with recombinant calpain 1 for 1, 2, 5 and 10 min and different peptide concentrations (pmol to µmol) (Fig. 3d). The generation of the YF13 (YRKSASTHHKSVF; 1547.7 Da) peptide was consistently observed in the presence of calpain, but not with the vehicle alone (DMSO) indicating the location of the calpain cleavage site of the human GPR50 between amino acid Phe-408 and Ser-409. A GPR50 construct deleted of its CTD at position 409 migrated at the same apparent molecular weight of 45 kDa as the N-terminal fragment generated upon cleavage of the CTD from the full-length GPR50 (Suppl Fig. 1c), further confirming the location of the calpain cleavage site at this position.

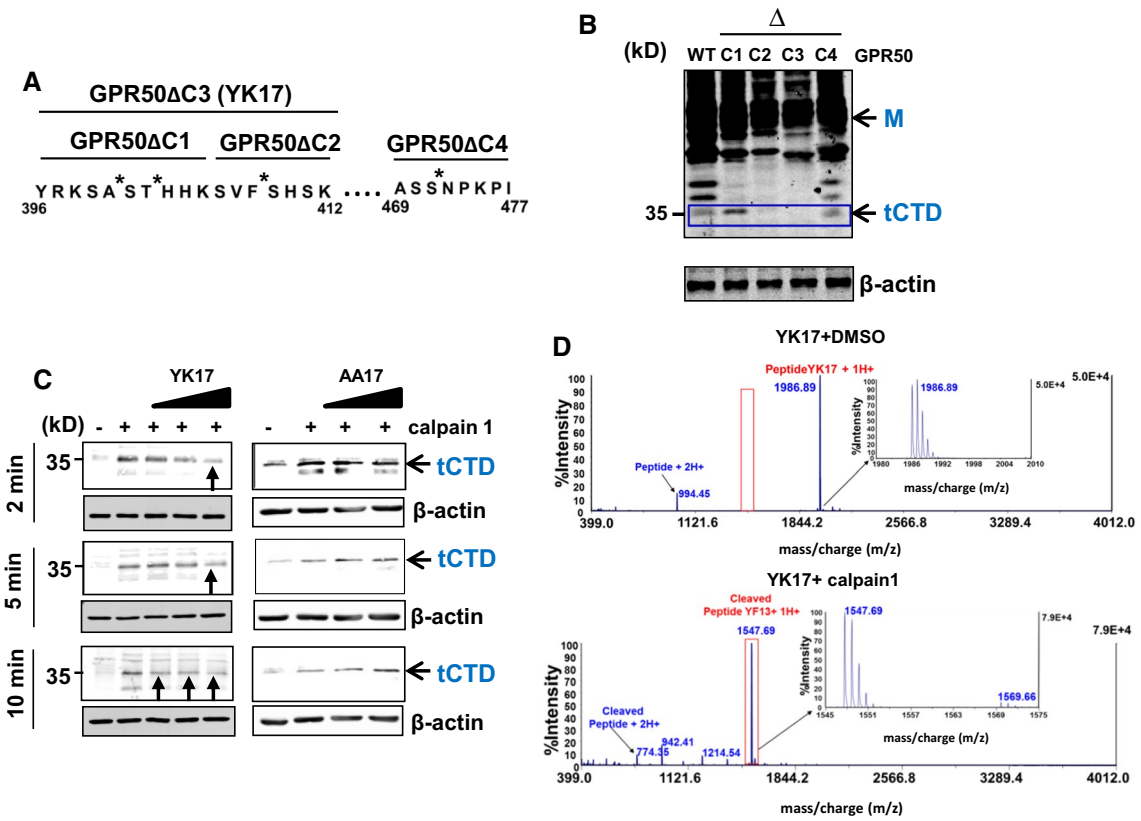

Fig. 3 Determination of calpain cleavage site of GPR50 by MALDI-TOF-MS. **a** Amino acid sequence surrounding four predicted calpain cleavage sites (asterisk) of GPR50. Deleted residues of the following GPR50 mutants are underlined (GPR50ΔC1: Δ396–405; GPR50ΔC2: Δ406–412; GPR50ΔC3: Δ396–412; GPR50ΔC4: Δ469–477). **b** Western blot showing tCTD in the indicated GPR50 wt and deletion mutants expressed in HEK293 cells. **c** Kinetics (2, 5, 10 min) of calpain 1 in vitro cleavage of GPR50 in the presence of 100 µM, 500 µM and 1 mM of peptide YK17 and 500 µM and 1 mM of peptide AA17 (control) in NCI-H520 cell lysates. Note: arrows showing reduction in cleavage at particular peptide concentration. **d** Display of MS spectrum obtained after MALDI-TOF-MS analysis of peptide YK-17 (YRKSASTHHKSVFSHSK; 1987.2 Da) with solvent (DMSO) alone (upper panel; at 1 µM of peptide) or with recombinant calpain 1 (lower panel; 1 U/mg) at 1 pmol of peptide. Peaks representing the detected peptide fragments with their respective molecular weight which was confirmed by sequencing and analysis. Red box in lower part shows the peak of cleaved fragment that correspond to YF13 (YRKSASTHHKSVF; 1547.7 Da) peptide. Representative results are shown for panels, **b**, **c**. Similar results were obtained in at least two additional experiments. See also Supplementary Fig. 3

Nuclear localization of the tCTD of GPR50

The release of the tCTD from the core domain of GPR50 raises questions about the subcellular localization of the tCTD in the cell. We studied the latter by confocal immunofluorescence (IF) microscopy expressing either the full-length GPR50, the GPR50ΔC2 construct or the tCTD alone (position 409–617) in HEK293 cells (Fig. 4a). Whereas the staining in full-length GPR50- and GPR50ΔC2-expressing cells was predominantly observed at the plasma membrane, the staining in Tctd-expressing cells was detected in the cytoplasm and highly enriched in the nucleus. Nuclear staining, although to a lesser extent, was also observed in full-length GPR50 but not in GPR50ΔC2-expressing cells. This observation is compatible with the partial cleavage of the full-length GPR50 in HEK293 cells. To confirm the nuclear localization of the tCTD, we performed subcellular fractionation studies. The tCTD was present in the nuclear fraction of cells expressing the isolated HA-tCTD or GPR50 full length and migrated at the expected size of 35 kDa (Fig. 4b). The presence of the tCTD in the nucleus was diminished in cells expressing the GPR50ΔC2 construct (Suppl Fig. 4a). Similar results were obtained in NCI-H520 cells expressing GPR50 endogenously (Fig. 4c). In these cells, the tCTD was even enriched in the nuclear fraction compared to the cytosolic fraction and a pretreatment with the calpain inhibitor ALLN, by decreasing tCTD cleavage, reduced the amount of nuclear tCTD as expected. Confocal microscopy of primary cultures of radial glial-like cells (tanycytes), known to express GPR50 abundantly [12], also showed significant nuclear immunoreactivity (Fig. 4d; Suppl Fig. 4b).

Nuclear translocation of proteins occurs by passive diffusion through nuclear pores with a size cutoff of ~ 40 kDa

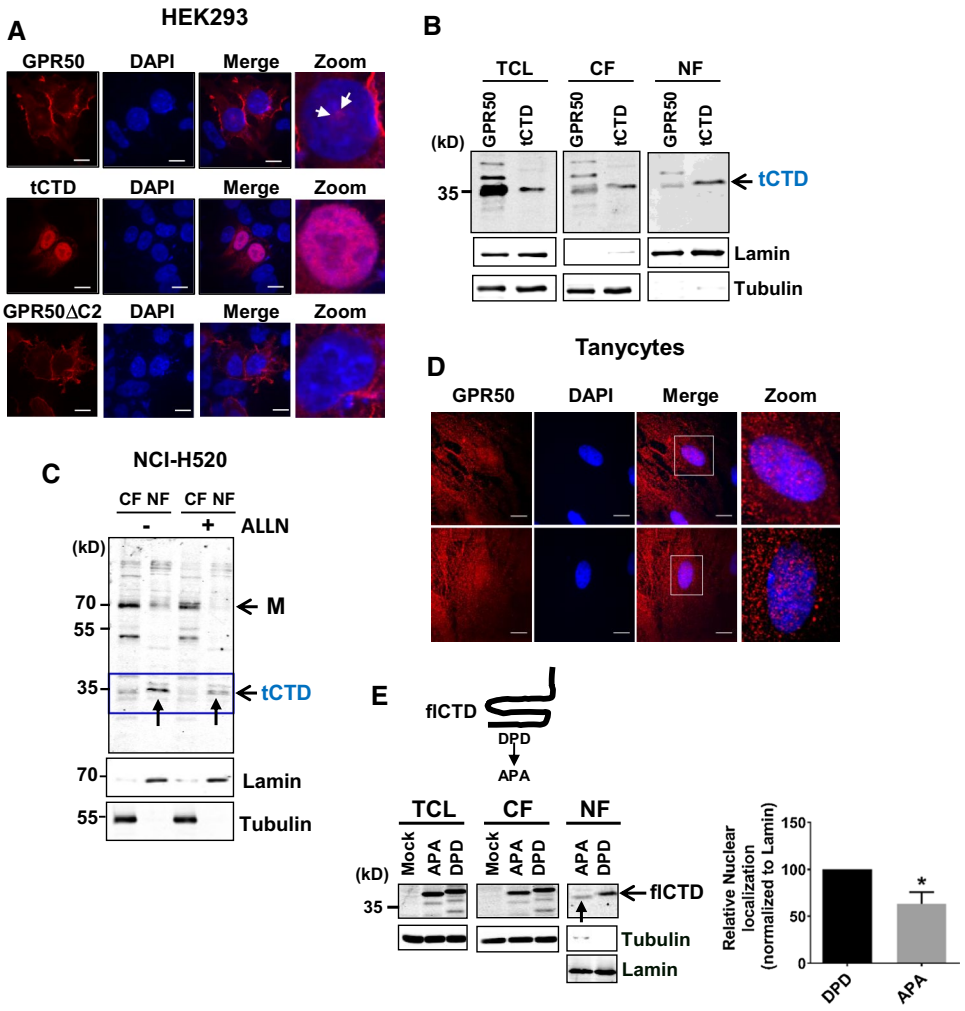

Fig. 4 Nuclear localization of the tCTD of GPR50. **a** Confocal images of HEK293 cells expressing either the full-length GPR50 (upper panel) showing staining at the cell membrane and nucleus (white arrows), the tCTD (middle panel) showing predominant nuclear staining and the GPR50ΔC2 construct showing staining at the cell membrane, but not the nucleus. GPR50 was stained with anti-GPR50 antibody, nuclei with DAPI (scale bar 10 µm). **b** Subcellular fractionation of HEK293 lysates of cells expressing either full-length GPR50 or tCTD showing nuclear localization of 35 kDa band (check arrow). **c** Subcellular fractionation of NCI-H520 cell lysates showing the nuclear localization of the 35 kDa band (tCTD) and its depletion (see arrow) in the presence of the calpain 1 inhibitor ALLN (10 µM, O/N). M, monomer of GPR50. **d** Confocal images of rat tanycytes stained with anti-GPR50 antibodies showing endogenous localization of GPR50. Zoom on nuclear localization. Staining of nuclei with DAPI (scale bar 10 µm). **e** Upper part: schematic representation of the flCTD of GPR50 and position of the 'DPD' motif mutated to APA; Lower part: Western blot showing reduced nuclear localization of APA flCTD. Quantification expressed as mean ± SEM, $n = 4$ independent experiments, $^{*}p < 0.05$ two-tailed unpaired Student's t test. Tubulin and lamin were used to detect the presence of cytosolic and nuclear proteins in different subcellular fractions. *TCL* total cell lysate, *CF* cytoplasmic fraction, *NF* nuclear fraction (panels **b**, **c**, **e**). Representative results are shown for panels **a**–**d**. Similar results were obtained in at least two additional experiments. See also Supplementary Fig. 4

and/or by specific signals such as the canonical nuclear localization signal (NLS). The tCTD of GPR50 does not contain any canonical NLS, but harbors a 'DPD' motif composed of two aspartate residues surrounding a proline residue that was shown to promote nuclear translocation of the extracellular signal-regulated kinase (ERK) [13]. Mutation of the two aspartate into alanine residues ('APA' motif) reduced the amount of the flCTD located in the nuclear fraction by approximately 40% (Fig. 4e). This suggests that the nuclear import of the tCTD occurs most likely through a combination of passive diffusion and the 'DPD' motif.

Collectively, these results indicate that a significant fraction of GPR50, most likely corresponding to the tCTD, is located in the nucleus in various cell types endogenously expressing GPR50. Nuclear import occurs through passive diffusion and is assisted by the 'DPD' motif present in the tCTD, although further mechanisms such as assisted transport, cannot be ruled out at the moment.

The tCTD of GPR50 interacts with the transcription factor TFII-I in the nucleus to promote c-fos promoter activation

To explore the function of the tCTD of GPR50 in the nucleus, we searched for GPR50-interacting partners by tandem affinity purification coupled to mass spectrometry and identified nine unique peptides in three independent experiments corresponding to the general transcription factor TFII-I in HEK293 cells stably expressing GPR50, but not in naïve HEK293 cells (Fig. 5a). The interaction was confirmed by coimmunoprecipitation (co-IP) experiments in GPR50-transfected HEK293 cells as well as in mouse brain lysates of wild-type mice, but not of GPR50KO mice (Fig. 5b). Immunoprecipitation of TFII-I revealed the presence of the GPR50 full length and tCTD in both HEK293 cell and mouse brain lysates, suggesting that TFII-I most likely interacts with the tCTD. The absence of co-IP in HEK293 cells expressing a GPR50 truncated of its CTD (GPR50TM-YFP) confirmed this hypothesis (Suppl Fig. 5a). Inversely, expression of the isolated tCTD was sufficient to detect the interaction with TFII-I by co-IP in the nuclear fraction of HEK293 cells (Fig. 5c). Colocalization of the tCTD with endogenous TFII-I in the nucleus of HEK293 cells is also consistent with an interaction occurring predominantly in the nucleus (Fig. 5d). GPR50 is highly expressed in tanycytes lining the third ventricle at the level of the hypothalamus [12, 14]. Colocalization between GPR50 and TFII-I was observed in mouse brain slices of tanycytes of wild-type mice (Fig. 5e), but not of GPR50KO mice (Suppl Fig. 5b). In primary cultures of tanycytes, the colocalization of GPR50 and TFII-I was strongest in the nucleus (Fig. 5f).

We took advantage of the well-characterized function of TFII-I in c-fos promoter transcriptional activity to study the role of GPR50 on gene transcription in NIH3T3 cells, known to show robust c-fos promoter activation [15]. Co-expression of a c-fos promoter construct either with the tCTD or the full-length GPR50 (WT or the frequent Δ4 human variant lacking four amino acids, 502TTGH505 (GPR50ΔTTGH) [16]) showed a marked c-fos activation that was similar to the effect of EGF treatment (Fig. 5g). Knock-down of TFII-I by siRNA completely abolished gene activation, demonstrating TFII-I dependence of the effect (Fig. 5g). No reporter gene activation was observed in cells expressing GPR50TM-YFP (lacking the CTD) or the GPR50ΔC2 mutant lacking the calpain cleavage site (Fig. 5g) or cells expressing the full-length GPR50 in the presence of the calpain inhibitor ALLN (Fig. 5h). Taken together, our results show that the tCTD in association with TFII-I regulates c-fos promoter activity.

RNA-Seq analysis reveals high DEG enrichment of transcriptional regulators.

To explore the impact of the tCTD on global gene transcription, transcriptomic profiling (RNA-sequencing) was performed in HEK293 cells stably expressing the tCTD vs. mock-transfected HEK293 cells (Mock). To obtain a representative and highly diverse mRNAs sample, mRNAs from four clones expressing the tCTD were mixed and compared to a pool of mock-transfected HEK293 cells. RNA-Seq data revealed a high number (~ 8000) of differentially expressed genes (DEG) ($p < 0.05$) spanning an expression range of more than four log 10 at modest tCTD expression levels (five times increase compared to background levels observed in mock cells) (Fig. 6a). Analysis of DEG with the Ingenuity pathway analysis (IPA) software revealed a significant ($p < 0.05$) enrichment of 78 canonical pathways in the dataset of the top 891 DEG analyzed (Suppl Table 1). Among the top five enriched canonical pathways, three were related to nuclear DNA damage/cell cycle/transcriptional regulation (GADD45 (growth arrest and DNA damage-inducible 45) signaling; aryl hydrocarbon signaling; p53 signaling) (Fig. 6b; Suppl Tables 2, 3, 4). This was further complemented by enrichment of two key transcriptional/cell cycle regulators (TP53 and ATF4) as top upstream regulators by the IPA software (Fig. 6c). Analysis of the molecular functions with the Gene Ontology software revealed 'transcription factor binding' as the top molecular function enriched in DEG ($p < 5.89E-05$) (Suppl Table 5). Analysis of DEG for the presence of predicted transcription factor binding sites in their promoter region with the Genomatix software revealed that 12 of the TOP-15 most significantly up-regulated and all of the TOP-15 most significantly down-regulated genes by the expression of the GPR50 tCTD contained the predicted TFII-I binding sites supporting the prominent role of this transcription factor in regulating target genes of the GPR50 tCTD (Suppl Table 6). GPR50 is reported to interact with and to activate the transcriptional coactivator TIP60 in the nucleus [8]. Consistently, we observed a significant upregulation of TIP60 and up/downregulation of its target genes (ATM, TBXT, ZEB1, etc.) in our tCTD sample ($p < 0.05$) (Fig. 6d). Taken together, our RNA-Seq data reveal that the tCTD modulates gene transcription at a large scale with enrichment of transcriptionally regulated pathways.

Discussion

We report here a novel signal transduction mode for GPCRs that relies on the proteolytic cleavage of its CTD. This signaling mode is fundamentally different from the canonical multistep GPCR signaling cascades involving G proteins/β-arrestins/second messengers and protein kinases

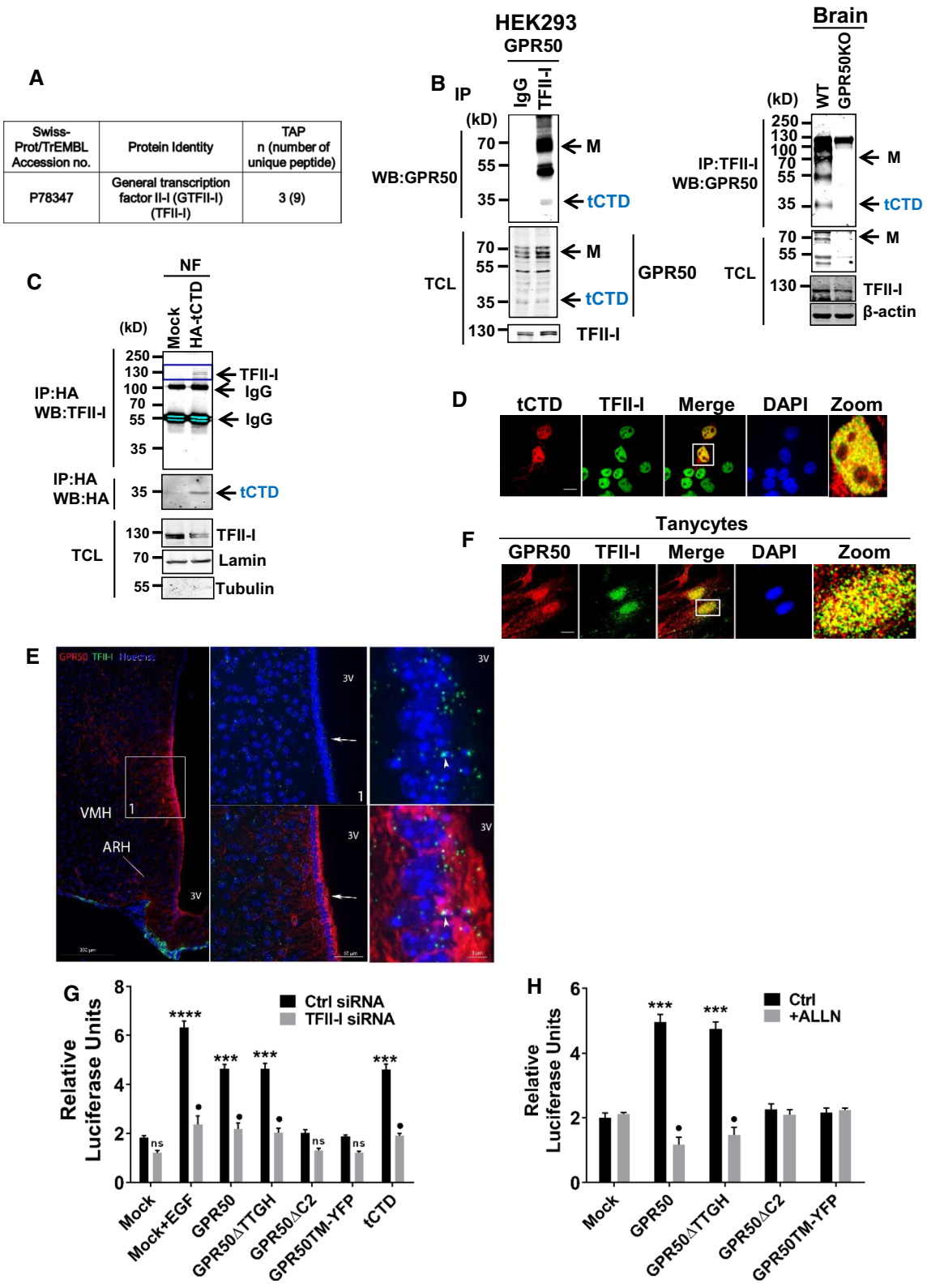

(Fig. 7). We show that the CTD of the orphan GPR50 is cleaved off from the GPR50 core by the calpain 1 protease in a Ca^{2+}-dependent manner between position 408 and 409, generating a truncated CTD (tCTD) of ~ 35 kDa that then translocates into the nucleus, most likely by passive diffusion and assisted by a nuclear translocation signal formed by a 'DPD' motif. In the nucleus, the tCTD modulates the expression of ~ 8000 genes of which many are involved in

◂**Fig. 5** The tCTD of GPR50 interacts with TFII-I in nucleus and promotes gene transcription. **a** Identification of the general transcription factor TFII-I by mass spectrometry after tandem affinity purification (TAP) of full-length GPR50 stably expressed in HEK293 cells. **b** Coimmunoprecipitation (co-IP) experiments in total cell lysates (TCL) of transfected HEK293 cells (left panel) and of mouse brain (right panel), respectively. TFII-I was immunoprecipitated and GPR50 revealed in precipitates by Western blot with anti-GPR50 antibody. Non-relevant IgG were used as a negative control in transfected cells and lysates of GPR50KO mice as negative control of brain samples. *M* GPR50 monomer, *tCTD* truncated C-terminal domain. **c** Co-IP experiment with the nuclear fraction (NF) of HEK293 cells expressing the HA-tagged tCTD. HA-tCTD was immunoprecipitated and TFII-I revealed in precipitates by Western blot. Mock-transfected cells were used as a negative control. The purity of the NF was verified by detecting laminin (nuclear) and tubulin (cytosolic). **d** Confocal images of nuclear colocalization of HA-tagged tCTD and endogenous TFII-I in HEK293 cells. Staining of nuclei with DAPI (scale bar 10 µm). **e**, **f** Confocal images of colocalization of GPR50 and TFII-I in mouse brain slices around the third ventricle region (3 V) (overview in the right panels and focus on the middle and left panels) and in primary rat tanycyte cultures (**f** scale bar 10 µm). Arrowheads show colocalization in panel **e**. Staining of nuclei with DAPI. *VMH* ventromedian hypothalamus, *ARC* arcuate nucleus. Reporter gene assay showing relative c-fos luciferase promoter activity ± silencing of TFII-I by siRNA (**g**) and ± ALLN (10 µM, O/N) (**h**) in NIH3T3 cells expressing full-length GPR50 (GPR50, GPR50ΔTTGH variant), GPR50TM-YFP (mutant lacking the CTD and fused to the yellow fluorescent protein (YFP)), GPR50ΔC2 (mutant lacking the calpain cleavage site) or the tCTD or in cells transfected with the empty vector (Mock). Values are expressed as mean ± SEM; $n = 3$ independent experiments; ****$p < 0.001$ and ***$p < 0.001$ vs. Mock Ctrl siRNA; •$p < 0.001$ significance of difference between Ctrl-siRNA vs. respective adjacent TFII-siRNA group; ns, non-significant difference (panel **g**); ***$p < 0.001$, significance of difference when compared to Mock Ctrl and •$p < 0.0001$, Ctrl vs ALLN of respective groups, (panel **h**), two-way ANOVA followed by Tukey's post hoc multiple comparison test. Representative results are shown for panels **b**–**f**. Similar results were obtained in at least two additional experiments. See also Supplementary Fig. 5

transcriptional regulatory networks. This is exemplified by the interaction and regulation of gene transcription associated with the general transcription factor TFII-I that is dependent on the proteolytic cleavage of GPR50 by calpains at position 408.

GPCRs are known to be primarily regulated by their respective natural ligand(s). Other prominent regulatory mechanisms include allosteric ligands and allosteric interactions with heterotrimeric G proteins, β-arrestins and various other interacting proteins and components of the phospholipid bilayer. Post-translational modifications are also a general regulatory trait of GPCRs ranging from reversible modifications such as phosphorylation, palmitoylation and glycosylation to irreversible modifications such as proteolysis. Autoproteolytic cleavage is observed for many adhesion GPCRs in the highly conserved GPCR proteolysis site (GPS) motif in the N-terminal extracellular domain [17]. Constitutive proteolytic cleavage occurs also in the extracellular ectodomain of the thyrotropin (TSH) receptor [18] and is integral part of the unique activation mechanism of the protease-activated receptor (PAR) family to generate the "tethered ligand" that activates the cleaved receptor [19]. Ligand-dependent proteolytic cleavage has been reported for the endothelin B [20] and vasopressin V2 receptors [21]. Proteolytic removal of the N-terminal domain of the alpha1D-adrenergic receptor and GPR37 has been shown to facilitate receptor surface expression [22, 23]. Cleavage of the intracellular CTD has been reported for the angiotensin II type 1 receptor AT1 [24] and the Dfrizzled2 GPCR [25], but remains poorly documented. Whether cleavage occurs at endogenously expressed AT1 receptors remains unknown. In the case of Dfrizzled2, the receptor was proposed to be first internalized into perinuclear compartments before the cleavage of the CTD and release into the nucleus. The proteases involved and the precise nuclear function remain unknown for both receptors.

Emerging evidence indicates that GPCR signaling cannot only occur at the plasma membrane, but also in intracellular compartments [26–28]. These signaling events typically rely on the classical cascades of G protein- or β-arrestin-dependent signal transduction. The proteolytic cleavage of the CTD of GPR50 described here is fundamentally different, as it relies on the cleavage of a receptor subdomain that then becomes the direct signal transducer from the plasma membrane to the nucleus. Whereas G protein-/β-arrestin-dependent signal transduction is based on a repeated activation/inactivation cycle with subsequent signal amplification, proteolytic cleavage of the CTD is irreversible and does not rely on amplification cascades. The concept of proteolytic liberation of intracellular receptor domains might be a general strategy of signal transduction from the cell surface to the nucleus as it has been reported for other membrane receptors such as Notch receptors, the amyloid precursor protein (APP), the receptor tyrosine kinase ErbB4, the multifunctional low-density lipoprotein receptor-related protein (LRP), and the cell-adhesion molecules CD44 [29–31]. Whereas the membrane-bound gamma-secretase seems to play a prominent role in the cleavage of the above-mentioned receptors, cytosolic calpains appear to be responsible for the cleavage of the CTD of GPR50. These Ca^{2+}-activated cysteine proteases regulate a wide range of cellular functions through the cleavage of their protein substrates including signal transduction-related molecules such as p35, IL1α, Myc oncoprotein and spectrin [32–34]. Calpain cleavage is a critical step in transforming the function and localization of its substrates in/out of the cytoplasm [34, 35]. Several lines of evidence indicate that GPR50 is cleaved at position 408 by calpain: (i) the cleavage of GPR50 is inhibited by calpain protease inhibitors, (ii) is dependent on intracellular Ca^{2+}, (iii) can be recapitulated by recombinant calpain 1, (iv) is inhibited by an excess of the inhibitory peptide

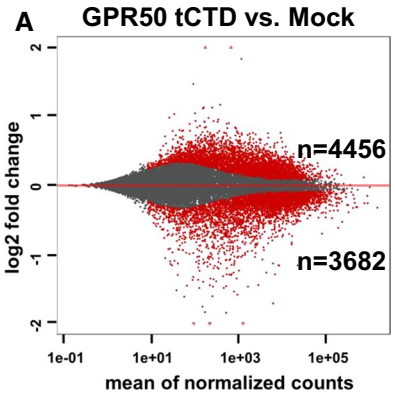

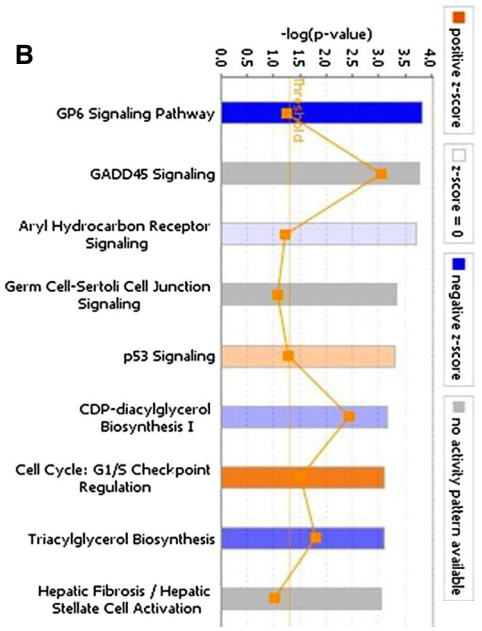

C

IPA: Top enriched upstream regulators

Upstream Regulator	p-value of overlap	Predicted Activation
TP53	2.43E-08	
hydrogen peroxide	6.93E-07	
NFKBIA	9.32E-08	
EGF	1.47E-06	Inhibited
ATF4	1.79E-06	Inhibited

IPA: Top enriched canonical pathways

Rank	Name	p-value	Overlap
1	GP6 Signaling Pathway	1.44E-04	13.0 % ; 17/131
2	GADD45 Signaling	1.73E-04	31.6 % ; 6/19
3	Aryl Hydrocarbon Receptor Signaling	1.90E-04	12.7 % ; 17/134
4	Germ Cell-Sertoli Cell Junction Signaling	4.64E-04	11.1 % ; 19/171
5	p53 Signaling	4.98E-04	13.1 % ; 14/107

D

TIP60 and related genes

Symbol	log2 fold change	p-value
TIP60	0.13	0.0078
ATM	0.26	8.15E-14
CREB1	0.19	6.32E-05
E2F8	0.25	3.09E-06
E2F3	0.15	1.39E-05
E2F4	-0.19	1.38E-05
STAT3	0.27	3.83E-08
TBXT	-1.01	3.48E-17
TBX19	0.47	7.37E-05
TBX18	0.12	0.0072
TBX2	-0.15	0.012
ZEB1	0.63	4.52E-49
TP53	0.21	5.75E-07
PARP3	0.34	3.23E-06

Fig. 6 Genome-wide modulation of gene transcription by the tCTD of GPR50. **a** MA—plot showing differentially expressed genes (DEG) in HEK293 cells expressing stably the tCTD vs. mock-transfected HEK293 cells, where *X*-axis represents the mean of normalized counts and the *Y*-axis displays log2 fold changes in DSeq2 RNA-Seq experiment. **b** The upper panel shows bar diagram of top canonical pathways predicted by Ingenuity pathway analysis (IPA) of DEG based on significant –log *p* values ($p < 0.05$). *Z* score represents overall predicted activation state of pathway in comparison to available literature (if positive: activated, orange shades; if negative: inhibited, blue shades; if no activity pattern or neutral, gray). The lower panel displays the top five pathways with percent and number of DEG overlapping with canonical pathway in IPA analysis. **c** List of top upstream regulators after IPA analysis based on significant *p* values (< 0.05) and their predicted mode of activation. **d** List of TIP60 and related genes enriched in the RNA-Seq dataset with significant *p* value (< 0.05). See also Supplementary Tables 1–6

encompassing the 408/409 cleavage site and (vi) is inhibited in GPR50 mutants devoid of the 408/409 cleavage site. Furthermore, the ~ 35 kDa cleavage fragment observed in mouse brain lysates and human lung carcinoma cells (NCI-H520) expressing endogenous GPR50 and in HEK293 cell expressing recombinant GPR50 (here and previous report [8]) migrate at an identical apparent molecular weight as the recombinant tCTD comprising amino acids 409–617.

Identification of the function of orphan receptors remains challenging in the absence of any ligand. The proteolytic cleavage of the CTD of GPR50 is of interest in this respect, as it proposes an alternative mechanism that, instead of relying on the activation state of the receptor ('receptor signaling' concept), relies on the availability of the receptor (GPR50) as a calpain substrate that would be regulated by the calpain activation status ('heterologous calpain signaling' concept). The latter hypothesis is supported by the observation that the soluble full-length CTD (flCTD) alone is a calpain substrate, suggesting that the GPR50 core domain is not mandatory for the generation of the tCTD. However, this does not exclude the possibility that the GPR50 core and its conformational modifications have an impact on the cleavage. The fact that spontaneous G protein (Gi and Gq) signaling of GPR50 appears not to be involved in GPR50 cleavage by calpain argues also against the 'receptor signaling' hypothesis, without however ruling out a potential role of a ligand-dependent GPR50 activation. Obviously, the 'receptor signaling' hypothesis will be difficult to prove in the absence of the ligand for GPR50. Supportive evidence for the 'receptor signaling' hypothesis comes from the observation that GPR50 cleavage is modulated in the presence of TβRI, a receptor known to interact

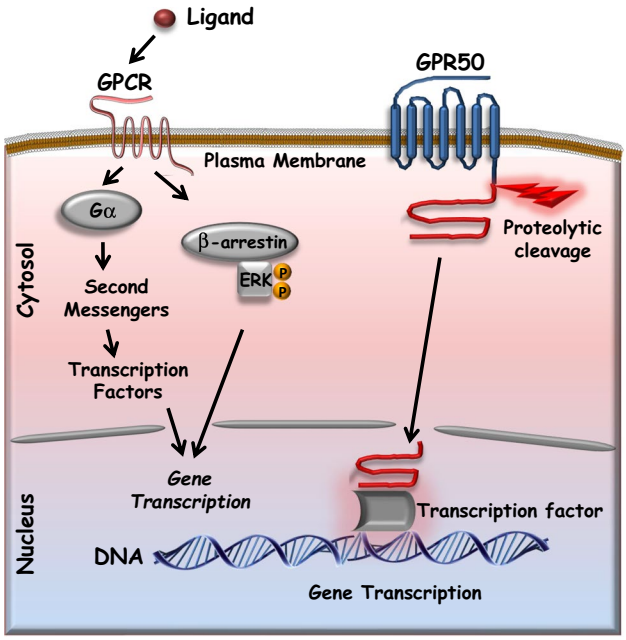

Fig. 7 Canonical and non-canonical signaling pathways of GPCRs. The canonical signal transduction mode of G protein-coupled receptors (GPCR) involves ligand binding and either G protein activation, second messenger generation and eventually the regulation and nuclear translocation of transcription factors or β-arrestin recruitment and ERK activation and nuclear translocation. The non-canonical signal transduction mode of GPR50 involves the proteolytic cleavage of its cytosolic carboxyl-terminal domain (CTD) and the direct translocation of the CTD into the nucleus where it interacts with transcription factors to regulate gene transcription

with GPR50 [5]. Indeed, co-expression of TβRI increases the generation of the tCTD with a further increase observed upon TGFβ stimulation. This result suggests that TβRI modulates the ability of calpain to cleave GPR50 through transconformational changes in the complex with GPR50. Future studies will address this interesting point. Whether the 'heterologous calpain signaling' exists for other orphan GPCRs remains elusive, but constitutes an interesting alternative signaling mode for this class of receptors that remains resistant to deorphanization [36].

Intriguingly, cleavage of the CTD of the human GPR50 not only generates a cytosolic fragment, but also generates a GPR50 core domain without the tCTD, which terminates after helix 8, located between N298 and F309 (see Suppl Fig. 3) generating a protein similar to the GPR50 homolog found in lower vertebrates [6]. Based on previous studies, the GPR50 core domain generated by cleavage of the CTD is likely to alleviate the allosteric inhibitory effect of GPR50 on MT_1 and TGFβ-RI receptor function in accordance with previous reports [4, 5].

Inspection of the sequence of the CTD of GPR50 uncovered a high homology with RNA polymerase II (RNAPolII), more precisely with its CTD. This domain is located outside of the catalytic core of the largest subunit of the RNAPolII and serves as a binding scaffold for numerous transcription factors. Accordingly, a similar function could be anticipated for the CTD of GPR50 [6]. To provide direct, experimental evidence for the functional role of the tCTD, we performed transcriptomic profiling of HEK293 cells expressing the tCTD and searched for interacting partners of GPR50 with the tandem-affinity approach. In agreement with the nuclear localization of the tCTD, a high number of differentially expressed genes (~8000) were observed which were enriched in transcription/cell cycle/DNA damage repair-related canonical pathways and as upstream regulators in ingenuity pathway analysis. Upregulation of TIP60 (KAT5) and its target genes in our data set was of particular interest, as GPR50 has been previously shown to interact with this histone acetylase and to enhance the co-activator property of glucocorticoid receptor signaling [8]. The effect of GPR50 on TIP60 function and expression is of particular interest since TIP60 fulfills several important functions in DNA damage repair and transcriptional and cell cycle regulation [37, 38].

Identification of the general transcription factor TFII-I as interacting partner of GPR50 is also fully consistent with the broad effect of the tCTD of GPR50 on gene transcription as observed in RNA-Seq. TFII-I is indeed ubiquitously expressed and is involved in the transcriptional activation of c-fos in response to extracellular mitogenic stimuli such as the epidermal growth factor (EGF) [15, 39] and regulates a number of diverse cellular processes [40]. TFII-I colocalized with the exogenously expressed tCTD in the nucleus of HEK293 cells and showed extensive colocalization in primary tanycyte cultures and in a discrete subset of tanycytes lining the third ventricle in mouse brain. The functional relevance of this physical interaction was shown in luciferase reporter gene assays under the control of the c-fos promoter. Full-length GPR50 and the tCTD alone, but not the GPR50 deletion mutant of the 408/409 cleavage site, enhanced c-fos promoter activation in a TFII-I- and calpain-dependent manner, demonstrating that the proteolytic cleavage of GPR50 at position 408/409 is necessary for transcriptional activation in the nucleus. The tCTD of GPR50 is likely to modulate c-fos gene expression in two ways: first, in a constitutive manner, proportional to GPR50 expression levels; second, in a dynamic manner either triggered by the activation of receptors modulating intracellular calcium levels or indirectly through the activation of receptors that by interacting with GPR50 could modify the ability of calpain to cleave GPR50. Our data indicate that these two modes of regulated signaling might indeed exist since ionomycin-mediated calcium influx and activation of the G_q/Ca^{2+} pathway by GPCRs as well as the activation of TβRI modulate GPR50 cleavage. Whether the regulated Ca^{2+}-dependent c-fos gene activation is strictly TFII-I dependent and whether it

involves previously identified intermediates such as CREB or ERK remains to be established [41–44].

The role of the tCTD is likely to go beyond the regulation of c-fos gene expression as indicated by the ~ 8000 differentially expressed genes in our RNA-Seq experiment including the previously described GPR50-interacting protein and transcriptional coactivator TIP60 [8]. It will be interesting to determine the impact of acute calcium regulation on a large scale, including the nature of the proteins modulating intracellular calcium concentrations such as calcium channels, NMDA receptor or GPCRs. If confirmed on a large scale, this mechanism could be a new non-canonical signaling mode of calcium-dependent gene regulation.

In conclusion, we report here an unconventional signaling mode of GPCRs that relies on the cleavage of the cytoplasmic receptor domain, which translocates to the nucleus and directly regulates gene transcription. This mechanism is reminiscent of that reported for other important membrane receptor families such as Notch, APP and ErbB4. Such an unconventional signaling mode offers the possibility of heterologous (ligand-independent) regulation by other cellular processes, a mechanism that is particularly interesting in the case of orphan receptors for which no ligands have been identified. The identification of a new and direct signal transduction mode of GPCRs, one of the largest receptor families, expands our understanding of signal transmission into the nucleus. The interaction of GPR50 with transcription factor points to a new and unexpected direct access of GPCRs to transcription regulation.

Materials and methods

Plasmids antibodies and reagents

Antibodies

GPR50 antibody7 was produced by Kernov Antibody Services [45]. Anti-lamin B (sc-6216; Santa-Cruz Biotech; 1/1000), anti-TFII-I (#4562; Cell signaling tech; 1/1000), anti-tubulin (MAB1864; Millipore; 1/2000), anti-HA monoclonal (16B12#MMS-101P; BioLegend; 1/1000), anti-HA (#3724, Cell signaling tech; 1/500), anti-flag (F7425; Sigma-Aldrich; 1/1000), anti-GFP (11,814,460,001; Roche; 1/2000), and anti-β-actin (MA5-15,739; Thermo Fisher; 1/2000) were used. All antibodies were used according to recommended dilutions for immunostaining, immunoprecipitation and Western blotting. c-fos-luciferase plasmid containing murine c-fos promoter (Kim et al. 1998) was a kind gift from Dr. Ananda L Roy (NIH, MD, USA). Calpain inhibitor-I (A6185, Sigma-Aldrich), calpain inhibitor II (A6060, Sigma-Aldrich), chloroquine (C6628, Sigma-Aldrich), recombinant human mu-calpain (C6108, Sigma-Aldrich), human EGF (E9644, Sigma-Aldrich) ALLN (208,719, Millipore), ALLM (208,721, Millipore), and rest of the protease inhibitors were bought from Sigma-Aldrich unless stated otherwise. Peptides YK17 and AA17 were synthesized and procured from Covalab (France) having 98% purity.

Cell culture and transfection and generation of stable cell lines

All media and chemicals were procured from Life Technologies, unless stated otherwise. HEK293/NIH3T3 cells were cultured in DMEM with 10% fetal bovine serum (FBS). Transient transfection was carried out by using Jet-Prime reagent (Polyplus-transfection) and Lipofectamine 2000 (Thermo Fisher). NCI-H520 (ATCC-HTB-182; human lung squamous cell carcinoma) cells were cultured in RPMI-1640 medium (GIBCO) with 10% FBS. Frozen rat tanycytes isolated from rat median eminences were cultured as previously described [46]. Cell lines were checked regularly for any mycoplasma contamination.

Stably GPR50 tCTD and empty vector (mock) overexpressing HEK293 cells were generated by jetPRIME Transfection of G418 resistant GPR50 plasmid. Selective pressure was established by using conditioned DMEM medium with 600 µg/mL G418 (Sigma-Aldrich). Further, monoclonal cell lines were obtained through a dilution limit process and positive clones expressing empty plasmid, GPR50 tCTD, were identified with Western blot.

Plasmid mutagenesis

Primers for point mutations were designed with the help of the Agilent QuikChange Primer Design program. Mutagenesis was performed by PCR with the Phusion High-Fidelity Polymerase (Finnzymes, Thermo-Fisher Scientific).

Western blotting

Cell lysates were mixed with Laemmli sample buffer (4×) and 100 mM DTT. 10–20 µg lysate for cells and 50 µg for tissue samples were separated on 10% or 12% SDS-PAGE and transferred onto nitrocellulose membrane overnight. After blocking for 1 h at room temperature in TBS with 0.1% Tween-20 (TBS-T) plus 5% skimmed milk powder, the membranes were incubated overnight at 4 °C with primary antibodies in TBS-T with 5% milk. Membranes were incubated with fluorescently tagged secondary antibodies (Life tech) in TBS-T for 30 min at room temperature and were washed for 3 × 5 min in TBS-T. Incubation with fluorescence-coupled secondary antibodies (Life technologies) enables readout on an Odyssey reader. For proteolytic cleavage experiments, HEK293 cells were treated with various

protease inhibitors such as serine/cysteine protease inhibitors (AEBSF 25 µM, E64 25 µM, leupeptin 50 µM, PMSF 50 µM), aspartic protease inhibitor (pepstatin 50 µM), calpain inhibitor I 10 µM, calpain inhibitor II 10 µM, proteasome inhibitor (MG132 10 µM, lactacystin 10 µM) and lysosomotropic agent, chloroquine (25 µM), following GPR50 transfection.

Co-immunoprecipitation

For preparation of cell lysates, cells were harvested after transfection in TNMG lysis buffer (20 mM Tris pH 8, 150 mM NaCl, 5 mM $MgCl_2$, 10% glycerol) with 1% NP-40 and solubilized on a wheel at 4 °C for 1 h, centrifuged at 14,000 rpm for 45 min and the supernatants were collected. Samples containing 1 mg protein were subjected to immunoprecipitation by incubating overnight with 2 µg of primary antibody. Protein G-sepharose beads (Sigma-Aldrich) were added to the lysate and incubated for 1 h at 4 °C. Beads were collected by centrifugation for 3 min at 3000 rpm and washed three times with lysis buffer (all at 4 °C). The precipitates were resuspended in 30 µl 2× Laemmli sample buffer with 100 mM DTT and boiled for 5 min. The supernatants were loaded on 12% SDS-PAGE gels and analyzed by Western blotting. For endogenous Co-IP, brain tissues were taken out from both, C57BL/6J wild-type and GPR50KO mice, homogenized and solubilized in 0.5% CHAPS detergent (Sigma-Aldrich) in TEM buffer (25 mM Tris pH 7.4, 2 mM EDTA, 10 mM $MgCl_2$) for 4 h at 4 °C on a wheel. The lysates were collected after centrifugation and subsequently used for immunoprecipitation. The protein estimation was performed with BCA kit (Thermo Fisher).

Immunofluorescence confocal microscopy

The transfected HEK293 cells were fixed in 4% paraformaldehyde for 15 min, permeabilized with 0.3% Triton X-100 for 10 min and blocked with a 5% horse serum/PBS solution. Cells were incubated overnight with primary antibody, fluorescent secondary antibodies were added, and slides were visualized by the use of a confocal microscope (Leica).

Immunostaining on perfused PAF 4% mouse brain sections was performed as reported previously [12]. Using a cryostat, 18-µm serial frozen sections were cut and collected on chrome–alum–gelatin-coated slides. Slide-mounted sections were processed for immunohistochemistry. Sections were rinsed four times in phosphate buffer saline (PBS) (pH 7.4) and blocked for 1 h using blocking solution (PBS containing 4% normal donkey serum and 0.3% Triton X-100) at 4 °C. Sections were incubated overnight at 4 °C with primary antibodies diluted in blocking solution (GPR50: Ac7, 1/750; TFII-I, Santa Cruz sc-9943, 1/100). The sections were then subjected to four washes in PBS and incubated for 1 h at room temperature with a mix of secondary Alexa Fluor-conjugated antibodies (1:500; Molecular Probes, Invitrogen) in the blocking solution. At the end of immunohistochemistry, the sections were coverslipped with 1,4-diazabicyclo[2.2.2]octane (Sigma-Aldrich).

Isolation of hypothalamaic tanycytes and endothelial cells using fluorescence-activated cell sorting

Median eminences from tat-cre-injected *td*Tomato$^{loxP/loxP}$ mice fed ad libitum ($n = 14$), were microdissected and enzymatically dissociated using Papain Dissociation System (Worthington, Lakewood, NJ) to obtain single-cell suspensions. This suspension was then incubated with Alexa Fluor 647 Rat Anti-Mouse CD31 clone 390 (BD Biosciences, ref: 563,608) for 45 min at 37 °C. FACS was performed using an EPICS ALTRA Cell Sorter Cytometer device (Beckman Coulter, Inc.). The sort was based on measurements of tdTomato fluorescence (excitation: 488 nm; detection: bandpass 675 ± 20 nm) by comparing cell suspensions from tdTomato-positive and wild-type animals and far red fluorescence (excitation: 633 nm; detection: bandpass 670 ± 30 nm) by comparing cell suspensions incubated with Alexa Fluor 647 Rat Anti-Mouse CD31 clone 390 and cell suspensions incubated with Alexa Fluor 647 Rat IgG2a, *k* isotype control (BD Biosciences, ref: 557,690). For each animal, 1000–4000 tdTomato positive cells and 1000 to 4000 far red positive cells were sorted directly into 10 µl extraction buffer: 0.1% Triton® X-100 (Sigma-Aldrich) and 0.4 U/µl RNaseOUT™ (Life Technologies).

Quantitative RT-PCR analyses

For gene expression analyses, mRNAs obtained from FACS-sorted cells were reverse transcribed using SuperScript® III Reverse transcriptase (Life technologies) and a linear preamplification step was performed using the TaqMan® PreAmp Master Mix Kit protocol (P/N 4,366,128, Applied Biosystems). Real-time PCR was carried out on Applied Biosystems 7900HT Fast Real-Time PCR System using exon boundary-specific TaqMan® Gene Expression Assays (Applied Biosystems): GPR50 (Gpr50-Mm00439147_m1); TFII-I (Gtf2i-Mm00494826_m1). Control housekeeping genes were r18S (rn18S-Mm03928990_g1); ACTB (Actb-Mm00607939_s1). Gene expression data were analyzed using SDS 2.4.1 and Data Assist 3.0.1 software (Applied Biosystem).

Tandem affinity purification

Tandem affinity purification (TAP) was performed as previously described [11]. Briefly, proteins were washed and

digested on calmodulin beads by trypsin for 3 h at 37 °C in 50 mM ammonium bicarbonate after reduction in 20 mM DTT at 60 °C for 30 min and alkylation in 50 mM iodoacetamide in the dark at RT for 30 min. The supernatant was collected for nLC MS/MS analysis and treated as described [47], but with the following settings for protein identification: extracted MS/MS peak lists were submitted to an in-house Mascot (Matrix Science), version 2.2, search engine. The Swiss-Prot database (April 28, 2008, 366,226 sequences; 132,054,191 residues) was used restricted to the Homo sapiens subset of sequences (19,372 sequences). Parent and fragment mass tolerances were, respectively, set to 100 ppm and 0.3 Da, and partial modification (oxidization) of methionine was allowed. Missed trypsin cleavage sites were limited to 1. A filter was applied to the search to reduce false positives and matching redundancies of the same peptide in several hits. All peptide matches above 1% risks of random matching were eliminated (p value < 0.01 filtering was applied). The individual minimum peptide score was set to 30. False-positive rates evaluated using Mascot. Identification were considered successful if at least two distinct peptides were identified. Under these stringent parameters, the minimum protein score was 29.

MALDI-TOF-mass spectrometric analysis

Peptide YK17 (YRKSASTHHKSVFSHSK; mol. wt. 1986 Da; 98% purified; water soluble; Covalab, France) having potential calpain cleavage site was incubated with calpain/DMSO in different concentration (pmol to µmol) and incubated at 30 °C at different concentrations (ranging from 1 pmol to 1 µmol). Aliquots of the samples were removed at various time intervals (1, 2, 5, 10, 15 min) and mixed 1:1 on a MALDI target plate with 5 mg of α-cyano-4-hydroxycinnamic acid matrix (Laser Biolabs) dissolved in 1 ml of 70% ACN 0.1% TFA 30% milliQ H_2O and allowed to dry on a 96-well OptiTOF MALDI plate target. Mass spectra were acquired at the 3P5 proteomics facility of the Université Paris Descartes with a 4800 MALDI-TOF/TOF analyser (ABSciex) with a 200 Hz Nd:YAG pulsed LASER (355 nm) shot frequency in positive reflectron mode at fixed fluency with low mass gate and delayed extraction. 500 spectra were summed by steps of 50 spectra in the range of 300–4000 Da. Monoisotopic values are labeled from isotope clusters with a minimal s/n ratio of 1000.

In vitro calpain cleavage assay

Total cell lysates (1 mg/mL) were incubated with recombinant human mu-calpain (1U/mg protein) in digestion buffer containing 50 mM Tris–HCl, pH 7.5, 5 mM β-mercaptoethanol, 100 mM NaCl and 100 µM $CaCl_2$ just before the reaction at 30 °C. Aliquots of the samples were removed at various time intervals (1, 2, 5, 10, 20, 30 and 45 min) and mixed immediately with equal volume of 6× Laemmli buffer (12% SDS, 60% glycerol, 0.6 mM DTT, 0.06% bromophenol blue) to terminate the digestion. The samples were boiled 5 min and used for gel electrophoresis and immunoblotting [48].

Calpain peptide competition assay

NCI-H520 cell lysates were incubated with different concentration of purified peptides (YK-17 and AA-17) before adding recombinant human calpain 1 (1 U/mg protein) in digestion buffer (50 mM Tris–HCl, pH 7.5, 5 mM β-mercaptoethanol, 100 mM NaCl, 100 µM $CaCl_2$) at 30 °C. The reaction was stopped at different time points (2, 5, 10 min.) by adding equal volumes of 6× Laemmli buffer (12% SDS, 60% glycerol, 0.6 mM DTT, 0.06% bromophenol blue). The samples were boiled for 5 min before loading onto SDS-PAGE.

Subcellular fractionation

Subcellular fractionation was done following the method published elsewhere [5, 49]. HEK 293 cells were seeded in 100 mm culture plates and transfected with the desired plasmids. The cells were harvested after 40 h of transfection. The culture plates were rinsed twice with ice-cold phosphate-buffered saline (PBS). Hypotonic buffer (500 µL) containing 1% NP-40 was added to each culture plate and allowed to swell on ice for 15 min. The cells were scraped and taken into fresh Eppendorf tube. The lysate was vortexed for 10 s, and the nuclei were pelleted (14,000 rpm for 1 min). The supernatant was collected as the cytoplasmic fraction. The nuclear pellets were resuspended in 100–200 µL of hypertonic buffer and rotated on a wheel for 45 min at 4 °C. This extract was then centrifuged (14,000 rpm for 30 min), and the nuclear fraction was collected. The amount of protein was estimated following BCA estimation kit (Thermo Fisher Scientific). The buffer compositions were as follows. (i) the hypotonic buffer contained 10 mM HEPES (pH 7.9), 10 mM KCl, 1.5 mM $MgCl_2$, 1 mM EDTA, 25 mM β-glycerophosphate, 1 mM Na_3VO_4 and 1 mM dithiothreitol (DTT); (ii) the hypertonic buffer contained 20 mM HEPES (pH 7.9), 420 mM NaCl, 1.5 mM $MgCl_2$, 25% glycerol, 1 mM EDTA, 25 mM β-glycerophosphate, 1 mM Na_3VO_4 and 1 mM DTT. To both buffers protease and phosphatase inhibitors were added just before use.

Reporter gene assay

NIH3T3 cells were maintained for 30 h in a medium containing 0.5% FBS following transfection and stimulated with hEGF (SRP3027, Sigma-Aldrich, 25 ng/mL) or 10% FBS

for 4 h before harvest. One hundred and fifty nanograms of c-fos-luc construct and 5 ng of pRL-TK for normalization and 250 ng of various GPR50 constructs were transfected per single well of a 12-well plate. The total amount of DNA per well was kept constant by adding empty plasmid pcDNA3 where necessary. For knocking down experiment of TFII-I, cells were transfected with siRNA against TFII-I and control siRNA by using Lipofectamine 2000 (Thermo Fisher). For calpain inhibitor (ALLN; 10 µM) experiment, cells were incubated O/N before harvest. All transfection experiments were performed in duplicate, and results were normalized to the expression of the *Renilla* luciferase transfection control. Lysis and measurement were performed with the Dual Luciferase Kit (Promega) according to the manufacturer's advices.

Generation of GPR50KO mice

The strategy used for GPR50KO mice generation has been explained and published elsewhere [5].

RNA isolation, library construction and transcriptome sequencing and analysis

The total RNA was extracted from mock and GPR50 tCTD ($n=3$ biological replicates) stably expressing HEK293 cells by using the TRIzol method (Life Technologies) and the concentrations were obtained using a fluorometric Qubit RNA HS assay (Life Technologies, Grand Island, New York, USA). The quality of the RNA (RNA integrity number 8.2) was determined on the Agilent 2100 Bioanalyzer (Agilent Technologies, Palo Alto, CA, USA) as per the manufacturer's instructions. To construct libraries, 1 µg of high-quality total RNA sample (RIN > 8) was processed using Truseq stranded mRNA kit (Illumina) as per manufacturer's instructions. Briefly, after purification of poly-A containing mRNA molecules, the mRNA molecules were fragmented and reverse- transcribed using random primers. Replacement of dTTP by dUTP during the second strand synthesis will permit achieving the strand specificity. Addition of a single A base to the cDNA was followed by ligation of adapters. Libraries were quantified by qPCR using the KAPA Library Quantification Kit for Illumina Libraries (KapaBiosystems, Wilmington, MA) and library profiles were assessed using the DNA High Sensitivity LabChip kit on an Agilent Bioanalyzer. Libraries were sequenced on an Illumina Nextseq 500 instrument using 75 base-lengths read V2 chemistry in a paired-end mode. After sequencing, a primary analysis based on AOZAN software (ENS, Paris) was applied to demultiplexer to control the quality of the raw data (based on FastQC modules/version 0.11.5). The obtained fastq files were then aligned using Star algorithm (version 2.5.2b) and quality control of the alignment was realized with Picard tools (version 2.8.1). Reads were then counted using feature count (version Rsubread 1.24.1) and statistical analyses on the read counts were performed with the DESeq2 package version 1.14.1 to determine the proportion of differentially expressed genes between two samples.

Data were analyzed through the use of Ingenuity pathway analysis, IPA (QIAGEN Inc., https://www.qiagenbioinformatics.com/products/ingenuity-pathway-analysis). Gene ontology, GO enrichment analysis, molecular functions (https://geneontology.org/) and Genomatix (https://www.genomatix.de/online_help/help_geps/gene-tf_analysis.html) softwares were also used for RNA-Seq data analysis.

Statistical analysis

Data were analyzed using GraphPad Prism 6 software (GraphPad software) and are presented as mean with SEM. The comparisons between two groups were performed using two-tailed unpaired Student's *t* test, while multiple groups were tested using analysis of variance (ANOVA) followed by Tukey's post hoc multiple comparison test. For RNA-Seq data, statistical analysis was performed with the DESeq2 package version 1.14.1 to determine the proportion of differentially expressed genes between two samples, and for complementary analysis with GO molecular functions, Fisher's exact test with FDR multiple test correction was used.

Acknowledgements We are grateful to Dr. Mark Scott (Institut Cochin, France) for expert advice and Cédric Broussard and Morgane Le Gall from the Plateform Protéomique 3P5 for protein identification by mass spectrometry and Franck Letourneur and Benjamin Saintpierre from the Genomic Facility of the Institut Cochin. This work was supported by grants from the Fondation Recherche Médicale (Equipe FRM 2006 to RJ), ARC No. NSFI20121205906, Agence Nationale de la Recherche (ANR-16-CE18-0013 to JD) and the "Who am I?" laboratory of excellence No.ANR-11-LABX-0071 funded by the French Government through its "Investments for the Future" program operated by The French National Research Agency under Grant No. ANR-11-IDEX-0005-01 (to RJ and RA), Inserm and CNRS.

Author contributions RA, OL, AS, JLG, PD, and RJ: conceptualization. RA, OL, AS, QZ, ML, SG, FG, and FL: investigation. FG, FL, VP, and PD: resources. RA and RJ: writing—original draft. RA, OL, SP, PD, JD, and RJ: writing—review and editing. PD, SP, JD, and RJ: funding acquisition. RA, OL, FG, FL, SP, VP, PD, JD, and RJ: supervision.

Compliance with ethical standards

Conflict of interest The authors declare no competing financial interests.

References

1. Weis WI, Kobilka BK (2018) The molecular basis of G protein-coupled receptor activation. Annu Rev Biochem. 87:897–919

2. Levoye A, Dam J, Ayoub MA, Guillaume JL, Jockers R (2006) Do orphan G-protein-coupled receptors have ligand-independent functions? New insights from receptor heterodimers. EMBO Rep. 7:1094–1098
3. Ahmad R, Wojciech S, Jockers R (2015) Hunting for the function of orphan GPCRs—beyond the search for the endogenous ligand. Br J Pharmacol. 172:3212–3228
4. Levoye A, Dam J, Ayoub MA, Guillaume JL, Couturier C, Delagrange P, Jockers R (2006) The orphan GPR50 receptor specifically inhibits MT(1) melatonin receptor function through heterodimerization. EMBO J. 25:3012–3023
5. Wojciech S, Ahmad R, Belaid-Choucair Z, Journe AS, Gallet S, Dam J, Daulat A, Ndiaye-Lobry D, Lahuna O, Karamitri A, Guillaume JL, Do Cruzeiro M, Guillonneau F, Saade A, Clement N, Courivaud T, Kaabi N, Tadagaki K, Delagrange P, Prevot V, Hermine O, Prunier C, Jockers R (2018) The orphan GPR50 receptor promotes constitutive TGFbeta receptor signaling and protects against cancer development. Nat Commun. 9:1216
6. Dufourny L, Levasseur A, Migaud M, Callebaut I, Pontarotti P, Malpaux B, Monget P (2008) GPR50 is the mammalian ortholog of Mel1c: evidence of rapid evolution in mammals. BMC Evol Biol. 8:105
7. Gautier C, Guenin SP, Riest-Fery I, Perry TJ, Legros C, Nosjean O, Simonneaux V, Grutzner F, Boutin JA (2018) Characterization of the Mel1c melatoninergic receptor in platypus (*Ornithorhynchus anatinus*). PLoS ONE 13:e0191904
8. Li J, Hand LE, Meng QJ, Loudon AS, Bechtold DA (2011) GPR50 interacts with TIP60 to modulate glucocorticoid receptor signalling. PLoS ONE 6:e23725
9. Ma YX, Wu ZQ, Feng YJ, Xiao ZC, Qin XL, Ma QH (2015) G protein coupled receptor 50 promotes self-renewal and neuronal differentiation of embryonic neural progenitor cells through regulation of notch and wnt/beta-catenin signalings. Biochem Biophys Res Commun. 458:836–842
10. Ould-Hamouda H, Chen P, Levoye A, Sozer-Topcular N, Daulat AM, Guillaume JL, Ravid R, Savaskan E, Ferry G, Boutin JA, Delagrange P, Jockers R, Maurice P (2007) Detection of the human GPR50 orphan seven transmembrane protein by polyclonal antibodies mapping different epitopes. J Pineal Res. 43:10–15
11. Daulat AM, Maurice P, Froment C, Guillaume JL, Broussard C, Monsarrat B, Delagrange P, Jockers R (2007) Purification and identification of G protein-coupled receptor protein complexes under native conditions. Mol Cell Proteom 6:835–844
12. Sidibe A, Mullier A, Chen P, Baroncini M, Boutin JA, Delagrange P, Prevot V, Jockers R (2010) Expression of the orphan GPR50 protein in rodent and human dorsomedial hypothalamus, tanycytes and median eminence. J Pineal Res. 48:263–269
13. Chuderland D, Konson A, Seger R (2008) Identification and characterization of a general nuclear translocation signal in signaling proteins. Mol Cell. 31:850–861
14. Drew JE, Barrett P, Mercer JG, Moar KM, Canet E, Delagrange P, Morgan PJ (2001) Localization of the melatonin-related receptor in the rodent brain and peripheral tissues. J Neuroendocrinol. 13:453–458
15. Ashworth T, Roy AL (2009) Phase specific functions of the transcription factor TFII-I during cell cycle. Cell Cycle 8:596–605
16. Thomson PA, Wray NR, Thomson AM, Dunbar DR, Grassie MA, Condie A, Walker MT, Smith DJ, Pulford DJ, Muir W, Blackwood DH, Porteous DJ (2005) Sex-specific association between bipolar affective disorder in women and GPR50, an X-linked orphan G protein-coupled receptor. Mol Psychiatry. 10:470–478
17. Nieberler M, Kittel RJ, Petrenko AG, Lin HH, Langenhan T (2016) Control of adhesion GPCR function through proteolytic processing. Handb Exp Pharmacol. 234:83–109
18. Rapoport B, McLachlan SM (2016) TSH Receptor cleavage into subunits and shedding of the A-subunit; a molecular and clinical perspective. Endocr Rev. 2016:23–42
19. Hamilton JR, Trejo J (2017) Challenges and opportunities in protease-activated receptor drug development. Annu Rev Pharmacol Toxicol. 57:349–373
20. Grantcharova E, Furkert J, Reusch HP, Krell HW, Papsdorf G, Beyermann M, Schulein R, Rosenthal W, Oksche A (2002) The extracellular N terminus of the endothelin B (ETB) receptor is cleaved by a metalloprotease in an agonist-dependent process. J Biol Chem. 277:43933–43941
21. Kojro E, Fahrenholz F (1995) Ligand-induced cleavage of the V2 vasopressin receptor by a plasma membrane metalloproteinase. J Biol Chem 270:6476–6481
22. Kountz TS, Lee KS, Aggarwal-Howarth S, Curran E, Park JM, Harris DA, Stewart A, Hendrickson J, Camp ND, Wolf-Yadlin A, Wang EH, Scott JD, Hague C (2016) Endogenous N-terminal domain cleavage modulates alpha1D-adrenergic receptor pharmacodynamics. J Biol Chem. 291:18210–18221
23. Mattila SO, Tuusa JT, Petaja-Repo UE (2016) The Parkinson's-disease-associated receptor GPR37 undergoes metalloproteinase-mediated N-terminal cleavage and ectodomain shedding. J Cell Sci. 129:1366–1377
24. Cook JL, Mills SJ, Naquin RT, Alam J, Re RN (2007) Cleavage of the angiotensin II type 1 receptor and nuclear accumulation of the cytoplasmic carboxy-terminal fragment. Am J Physiol Cell Physiol. 292:C1313–C1322
25. Mathew D, Ataman B, Chen J, Zhang Y, Cumberledge S, Budnik V (2005) Wingless signaling at synapses is through cleavage and nuclear import of receptor DFrizzled2. Science 310:1344–1347
26. Vilardaga JP, Jean-Alphonse FG, Gardella TJ (2014) Endosomal generation of cAMP in GPCR signaling. Nat Chem Biol. 10:700–706
27. Tsvetanova NG, Irannejad R, von Zastrow M (2015) G protein-coupled receptor (GPCR) signaling via heterotrimeric G proteins from endosomes. J Biol Chem. 290:6689–6696
28. Jong YI, Harmon SK, O'Malley KL (2017) GPCR signalling from within the cell. Br J Pharmacol. https://doi.org/10.1111/bph.14023
29. Fortini ME (2002) Gamma-secretase-mediated proteolysis in cell-surface-receptor signalling. Nat Rev Mol Cell Biol. 3:673–684
30. Sardi SP, Murtie J, Koirala S, Patten BA, Corfas G (2006) Presenilin-dependent ErbB4 nuclear signaling regulates the timing of astrogenesis in the developing brain. Cell 127:185–197
31. Selkoe D, Kopan R (2003) Notch and Presenilin: regulated intramembrane proteolysis links development and degeneration. Annu Rev Neurosci. 26:565–597
32. Seo J, Giusti-Rodriguez P, Zhou Y, Rudenko A, Cho S, Ota KT, Park C, Patzke H, Madabhushi R, Pan L, Mungenast AE, Guan JS, Delalle I, Tsai LH (2014) Activity-dependent p25 generation regulates synaptic plasticity and Abeta-induced cognitive impairment. Cell 157:486–498
33. Kobayashi Y, Yamamoto K, Saido T, Kawasaki H, Oppenheim JJ, Matsushima K (1990) Identification of calcium-activated neutral protease as a processing enzyme of human interleukin 1 alpha. Proc Natl Acad Sci U S A. 87:5548–5552
34. Conacci-Sorrell M, Ngouenet C, Eisenman RN (2010) Myc-nick: a cytoplasmic cleavage product of Myc that promotes alpha-tubulin acetylation and cell differentiation. Cell 142:480–493
35. Gross O, Yazdi AS, Thomas CJ, Masin M, Heinz LX, Guarda G, Quadroni M, Drexler SK, Tschopp J (2012) Inflammasome activators induce interleukin-1alpha secretion via distinct pathways with differential requirement for the protease function of caspase-1. Immunity 36:388–400
36. Davenport AP, Alexander SP, Sharman JL, Pawson AJ, Benson HE, Monaghan AE, Liew WC, Mpamhanga CP, Bonner TI, Neubig RR, Pin JP, Spedding M, Harmar AJ (2013) International

Union of Basic and Clinical Pharmacology. LXXXVIII G protein-coupled receptor list: recommendations for new pairings with cognate ligands. Pharmacol Rev. 65:967–986
37. Squatrito M, Gorrini C, Amati B (2006) Tip60 in DNA damage response and growth control: many tricks in one HAT. Trends Cell Biol. 16:433–442
38. Ikura T, Ogryzko VV, Grigoriev M, Groisman R, Wang J, Horikoshi M, Scully R, Qin J, Nakatani Y (2000) Involvement of the TIP60 histone acetylase complex in DNA repair and apoptosis. Cell 102:463–473
39. Kim DW, Cheriyath V, Roy AL, Cochran BH (1998) TFII-I enhances activation of the c-fos promoter through interactions with upstream elements. Mol Cell Biol. 18:3310–3320
40. Roy AL (2007) Signal-induced functions of the transcription factor TFII-I. Biochim Biophys Acta. 1769:613–621
41. Lerea LS, Butler LS, McNamara JO (1992) NMDA and non-NMDA receptor-mediated increase of c-fos mRNA in dentate gyrus neurons involves calcium influx via different routes. J Neurosci. 12:2973–2981
42. Xia Z, Dudek H, Miranti CK, Greenberg ME (1996) Calcium influx via the NMDA receptor induces immediate early gene transcription by a MAP kinase/ERK-dependent mechanism. J Neurosci. 16:5425–5436
43. Kim DW, Cochran BH (2000) Extracellular signal-regulated kinase binds to TFII-I and regulates its activation of the c-fos promoter. Mol Cell Biol. 20:1140–1148
44. Thomas GM, Huganir RL (2004) MAPK cascade signalling and synaptic plasticity. Nat Rev Neurosci. 5:173–183
45. Hamouda H, Chen P, Levoye A, Sözer-Topçular N, Daulat A, Guillaume J, Ravid R, Savaskan E, Ferry G, Boutin J, Delagrange P, Jockers R, Maurice P (2007) Detection of the human GPR50 orphan seven transmembrane protein by polyclonal antibodies mapping different epitopes. J Pineal Res. 43:10–15
46. Prevot V, Cornea A, Mungenast A, Smiley G, Ojeda SR (2003) Activation of erbB-1 signaling in tanycytes of the median eminence stimulates transforming growth factor beta1 release via prostaglandin E2 production and induces cell plasticity. J Neurosci. 23:10622–10632
47. Andre W, Nondier I, Valensi M, Guillonneau F, Federici C, Hoffner G, Djian P (2017) Identification of brain substrates of transglutaminase by functional proteomics supports its role in neurodegenerative diseases. Neurobiol Dis. 101:40–58
48. Garg S, Timm T, Mandelkow EM, Mandelkow E, Wang Y (2011) Cleavage of Tau by calpain in Alzheimer's disease: the quest for the toxic 17 kD fragment. Neurobiol Aging. 32:1–14
49. Wong C, Rougier-Chapman EM, Frederick JP, Datto MB, Liberati NT, Li JM, Wang XF (1999) Smad3-Smad4 and AP-1 complexes synergize in transcriptional activation of the c-Jun promoter by transforming growth factor beta. Mol Cell Biol. 19:1821–1830